Dimensional Control and Formability in Impact Forming

S. Srinivasan[1], H.Wang[1], G.A.Taber[1] and G. S. Daehn[1]

[1] Ohio State University 2041 College Rd, Columbus, Ohio, USA

Abstract

Electromagnetic forming (EMF) is a high speed forming technique that can be used for embossing fine surface features onto sheet metals. Here two coupled experimental and analytical studies show how interface conditions including rebound and friction affect the ability to create a component in impact forming. In the first part of this work high velocity is generated with the Uniform Pressure Actuator (UPA) and impact with a die emboss fine features in a nominally flat component. The primary objective of this work is to develop a modelling facility that guides experimental design nominally flat grooved components. Both shape fidelity and formability aspects are presently considered. In a second short study expansion of a round tube into a square hole is considered. Traditional modelling techniques solve a coupled system of equations with spatially varying electromagnetic fluxes controlling the dynamics of the plastic deformation. Because the magnetic pressure is spatially uniform, the flux equations are obviated from the coupled system rendering them computationally efficient. The calibration of contact mechanics that influence the rebound behaviour of the sheet metal remains as a difficult issue. The interfaces between various sheet metals and the metal die play a critical role in controlling the shape of the final product. The characterization of such an interface using appropriate calibrated friction coefficients is assessed. The role of magnetic pressure in reducing the sheet metal rebound is demonstrated via a comparison between results from mechanical and electromagnetic simulations. The influence of the channel geometry on final shape is illustrated through simulation and experiments.

Keywords

Electromagnetic forming, Numerical Simulation, Constitutive behaviour

1 Introduction

Electromagnetic forming uses the magnetic repulsion between two very large opposing currents to form sheet metal [1]. The punch is eliminated from the assembly and the sheet metal is driven into the die by its own inertia. Typical primary currents on the order of 100 kA with rise times of about 10μs are common and velocities within the range of 100-300 m/s are often achieved. The current investigation concerns high speed forming for the manufacture of grooved nominally flat plates. Understanding both the correspondence between the die shape and final part shape and ability to make the part without sheet rupture are paramount in a successful forming operation.
This study will consider two kinds of problems, first a more complex one dealing with the manufacture of a nominally flat plate with semi-circular grooves (Section 2). This will point out the need for simpler, more tractable problems. That motivates the much simpler, but still illuminating study of expansion of the proverbial round tube into a square hole that is considered in Section 3.

2 Impact Forming of Grooved Plates

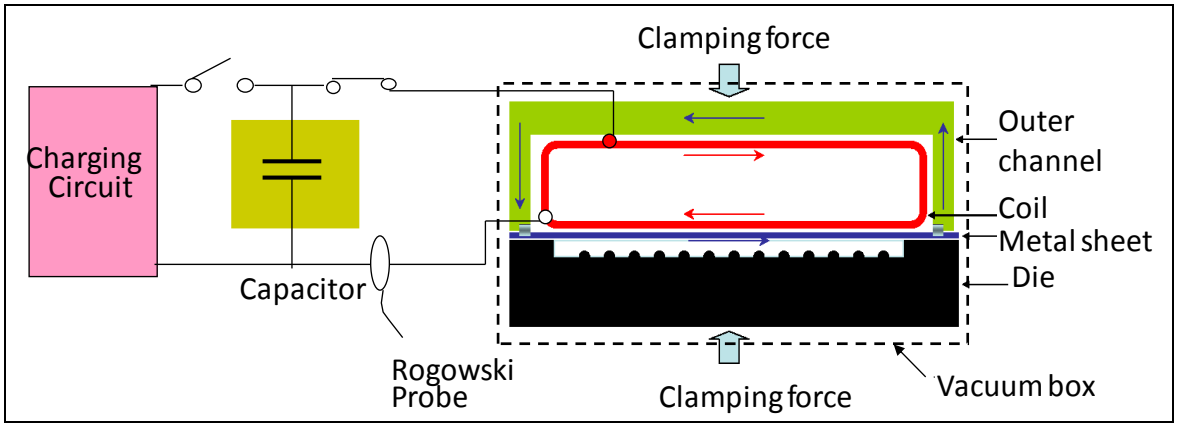

Figure 1: *Schematic of electromagnetic forming for grooved plates (Kamal & Daehn, 2007)*

2.1 Experimental Setup

The experiment system consists of a 16 kJ capacitor bank, helical copper coil, uniform pressure coil, a cylindrical casing, a flat box casing, a square metal die cavity (2.25 inches), aluminium rings of inner radius 24 mm, width 10 mm and thickness 1.3 mm. The primary copper coil is embedded inside the casing by cast tooling grade urethane. The ring or sheet specimen as the case may be, sits on the casing to complete the secondary circuit. The separation distance between the specimen and the die is 3 mm. Figure 1 shows that a high electrical discharge from the capacitor bank charges the primary circuit embedded in the coil box. The primary current induces a secondary current in the metal blank. The two currents being opposite in nature generate repulsion high enough to drive the ring into the die. A photon Doppler velocimeter system [2] is used to measure velocities of the accelerating specimen. The overall utility, design and behavior of this UPA forming system have been described by Kamal [1] and Banik [6] previously.

2.2 Constitutive Models

Titanium sheets of thickness 0.003" were formed into a steel die with fine semicircular channels with depths of the order of 0.015 inches as shown in Figure 2. A copper driver sheet of thickness 0.006" was used to complete the secondary circuit owing to its high electrical conductivity. The copper driver provides pressure to the titanium sheet during the forming process, accelerating it and co-deforming with the titanium. The forming is accomplished under vacuum to eliminate the resistance to forming due to compressed air. The strain distributions from the simulation model have been superimposed on the experimental measurements in Figure 2. The simplified Johnson and Cook (J-C) model [3] as shown in equation (1) was selected to characterize the material behavior. This form was chosen for its relative simplicity and the absence of a clearly better simple model [4]. For simplicity, the influence of temperature on the flow stress was neglected [5]. The J-C form is represented as:

$$\sigma_y = \left(A + B\,\varepsilon^n\right)\left(1 + c \ln \dot{\varepsilon}\right) \tag{1}$$

Where σ_y represents the flow stress (applied force per unit area), *A* is the yield stress (transition from elastic to plastic regime), *B* and *n* are parameters corresponding to the strain hardening law, *c* is the strain-rate parameter, ε is the effective plastic strain, and $\dot{\varepsilon}$ is the strain-rate. The simplified failure law of Johnson-Cook involves a characteristic parameter i.e. the effective (von-Mises criterion) plastic strain at fracture (ε_f) shown in (2). Numerically, this implies that if the average strain (von-Mises criterion) in any grid element is greater than fracture strain then the element is deleted from the simulation.

$$\bar{\varepsilon} \geq \bar{\varepsilon}_f \qquad at\ failure \tag{2}$$

The strain rate sensitivity was used as an optimization parameter and its values are tabulated in *Table 1*.

2.3 Simulation

Simulations are carried out in the fully explicit simulator LS-DYNA. The boundary condition for the simulation is set using the magnetic pressure on the driver plate. This magnetic pressure is calibrated using the velocity of the flyer measured from the experiments using the PDV system described in section 2.1.

Specimen	A (MPa)	B (MPa)	n	*c*
Copper driver	100	150	0.3	0.06
Titanium	200	700	0.22	0.06
Steel (Die)	20	550	0.05	0.05

***Table 1**: Johnson-Cook parameters for titanium specimen and copper driver*

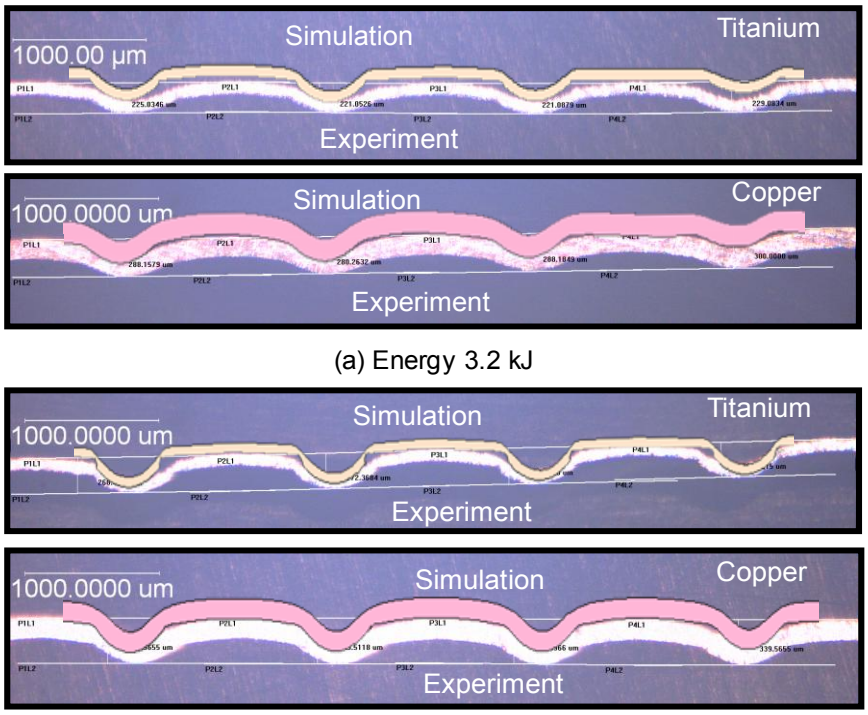

(a) Energy 3.2 kJ

(b) Energy 6.4 kJ

Figure 2: *Deformed specimens of titanium sheet and copper driver at two energies*

3 Effect of Friction on Quality of Formed Workpiece

3.1 Experimental Setup

The experiment system is identical to the one described in section 2.1. Experiments were conducted with austenitic stainless steels SS201 (instead of Titanium) and copper was used as a driver. *Figure 3* shows comparison between model and experiments for the SS201 sheets. The comparison for copper sheets is not shown. The same metal die described in section 2.1 was used. A lubricant such as boron nitride was used to study frictional effects on interfaces [6].

3.2 Mechanics

The contact interface between the two metal sheets and the die influences the impact dynamics and strongly affects local strain accumulation. It governs the efficiency of load transfer between components involved in the impact. Under normal conditions the frictional coefficient is high and ensures efficient load transfer between interfaces. This gives relatively uniform strain distributions. With the addition of lubricant, the friction coefficient is reduced and the propensity of relative lateral motion between the components is enhanced. This tends to cause strain localization at the die corners. Figure 3(b) shows that when lubrication is applied only between SS201 and the die there isn't very efficient transfer of energy between SS201 and the die. There is however good energy transfer between copper and SS201. This implies that a large proportion of the energy is absorbed by SS201 and thus there are 3 fractured zones. Figure 3(c) shows that when lubrication is applied on all surfaces large amount of the impact energy is absorbed

by copper driver (towards plastic flow and heating). A lower amount than in the cases of (a) and (b) is transferred onto SS201 or the die.

3.3 Simulation

The boundary conditions used in this model were identical to section 2.3. The pressure condition is calibrated against experimentally evaluated velocities (PDV system). The friction conditions in LS-DYNA factor in the contact cards that are used to describe the interface conditions. The CONTACT_AUTOMATIC_SURFACE_TO_SURFACE keyword was used to simulate all the interfaces (Details available in LS-DYNA manual 2006, http://lstc.com/manuals.htm). The Coulombic friction co-efficient was used in the simulation as shown in equation (3) below. The static and dynamic friction coefficients under normal conditions were 0.5 and that with lubrication were 0.05. The decay co-efficient was set to 0.1 for all cases.

$$\mu_{eff} = \left(\mu_{dynamic} + \left(\mu_{static} - \mu_{dynamic}\right) \bullet \left(e^{-\alpha \Box v_{rel}}\right)\right)$$
$$\mu_{eff} = \text{Effective frictional coefficient}; \alpha = \text{decay coefficient}$$
$$v_{rel} = \text{relative velocity between contacting bodies} \qquad (3)$$

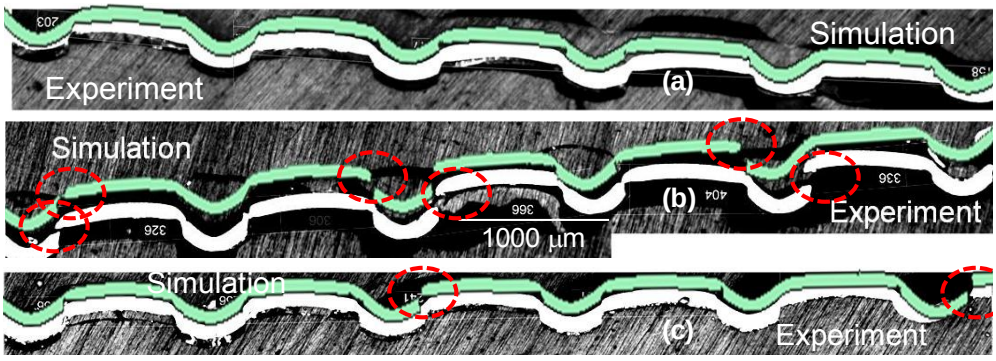

Figure 3: *Deformed specimens of SS201 sheet from simulation and experiment (Energy 4.8 kJ) (a) No lubrication (b) Lubrication between SS201 and Die (c) Lubrication on all interfaces*

Figure 3 only shows the comparison between experimental and model for austenitic steels SS201. The copper driver is not shown since SS201 is the product of concern. It is clear that the second case where lubrication is applied only between copper and SS201 has the maximum damage induced on the specimen. This is counterintuitive. The traditional expectation is that adding lubricants between interfaces prevents failure or damage and friction is often considered detrimental to the final product. However, under high speed conditions, it seems like the absence of friction is detrimental to the product shape and quality.

4 Constrained Ring Expansion

4.1 Objective

Experimental work in forming shallow pans with the UPA and similar driver systems has demonstrated that dimensional irregularities, failure and 'ghost lines' can often form away from the corners. A good example of this can be seen in [7]. Here a simple prototypical problem is considered and the numerical finite element model is validated against the experimental strain distributions and velocity measurements.

4.2 Experimental Setup

A circular aluminum ring was expanded into a steel square die. The experiment uses a 16 kJ capacitor bank (at maximum charging voltage of 8.66 kV), 5 turn helical copper coil, a cylindrical casing of outer radius 24 mm, a square metal die cavity (2.25 inches), aluminum rings of inner radius 24 mm, width 10 mm and thickness 1.3 mm. The primary copper coil is embedded inside the cylindrical casing by means of tooling grade urethane. The ring fits onto the casing to complete the secondary circuit. The standoff distance between the ring and the die cavity is 3 mm. Discharge from the capacitor bank charges the primary circuit embedded in the coil box. The primary current induces a secondary current in the metal blank. The two currents being opposite in nature generate repulsion high enough to drive the ring into the die.

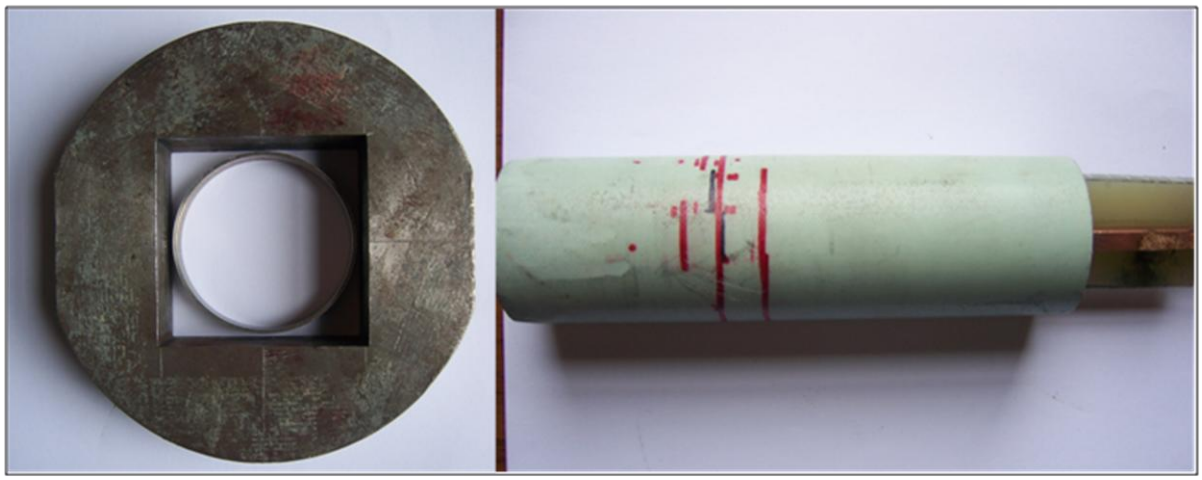

Figure 4: *Experimental setup of electromagnetic ring expansion (a) Square die (b) Helical coil*

4.3 Simulation

The traditional modeling algorithm [8] is divided into two coupled parts; electromagnetic flux equations and the mechanics governing plastic flow. The measured current from the capacitor bank sets the initial condition to the simulator. The entire system of equations is solved by the electromagnetic version of LS-DYNA [9]. In the subsequent cases, the electromagnetic component of the system of equations is excluded and a magnetic pressure boundary condition is applied to the ring. This method is identical to the sections described above. The pressure boundary condition is released at the onset of impact to let the ring flow plastically on account of its own inertia. The plastic strain at fracture as

described in equation (2) is inferred empirically from the relative change in cross sectional areas of the sheet metal specimen before and after impact. Two velocities were measured in the directions shown in *Figure 5* (b).

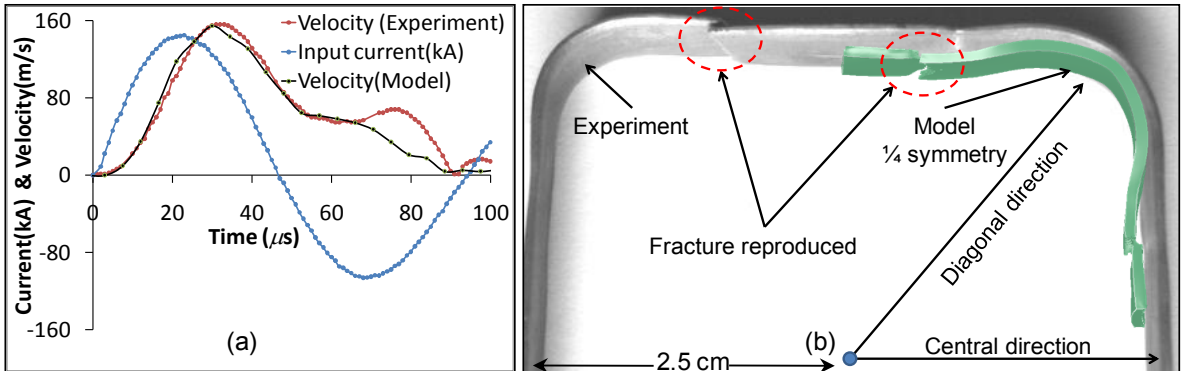

Figure 5: *(a) Input current and output velocity (b) Model vs. ring expansion experiments @ 5.6 kJ*

Figure 5 & *Figure 6* show the input current, the experimental and simulated impact velocities (along the diagonal direction only) and the comparison between the ring configurations after impact at two energies. The magnetic pressure (single constant value), inferred from the input current sets the input condition to the simulation. The impact velocities measured at two locations on the ring circumference in both the indicated directions help were used to calibrate the model. Both the simulations and experiment shows reduced propensity for failure at the higher impact energy. This is presumably because the sample strikes the die more uniformly [10]. Both the simulations and model show that there is a rebound phenomenon that produces a component that is far from square in the end and these rebounds drive the failure process.

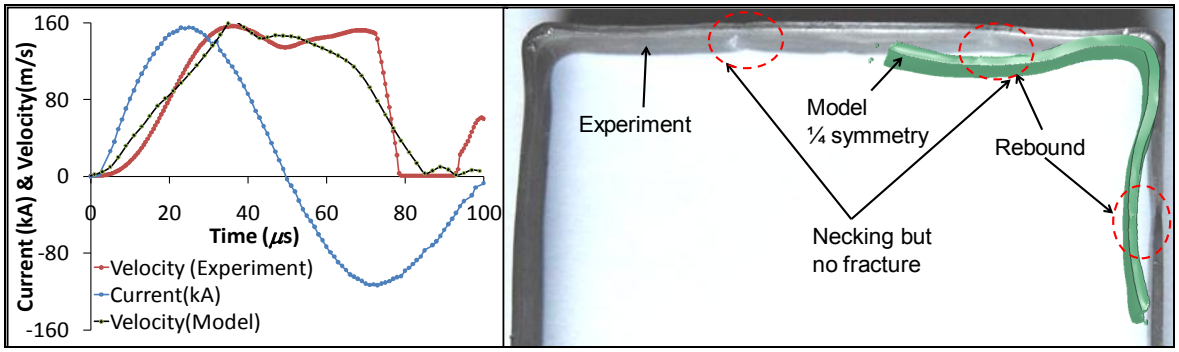

Figure 6: *(a) Input current and output velocity (b) Model vs. ring expansion experiments @ 7.2 kJ*

4.4 Results

In part (1) of *Figure 7*, as the ring strikes the square die, it rebounds and undergoes a rapid change in stress states (tensile to compressive in the circumferential direction). Meanwhile, the magnetic pressure causes the ring to advance in the diagonal direction. The intermediate region between the central and diagonal direction acts like a tensile

specimen. It necks and consequently fails under influence of a multiaxial stress states [11]. There is a complicated interaction between stress waves travelling towards each other as shown in *Figure 7*. In this process there is a strong interaction between the wave fronts subsequently followed by their energy dissipation (Part (2)). Part (4) shows the stress release upon fracture. The final shape of the product is not exactly the same as the square die. This is largely attributed to rebound of the ring from the edge of the die. There is a distinct similarity observed in the fracture paths from the simulation model and the experiments shown in Figure 8. Part of the kinetic energy of the ring has to be plastically dissipated in order to minimize the bounce-off.

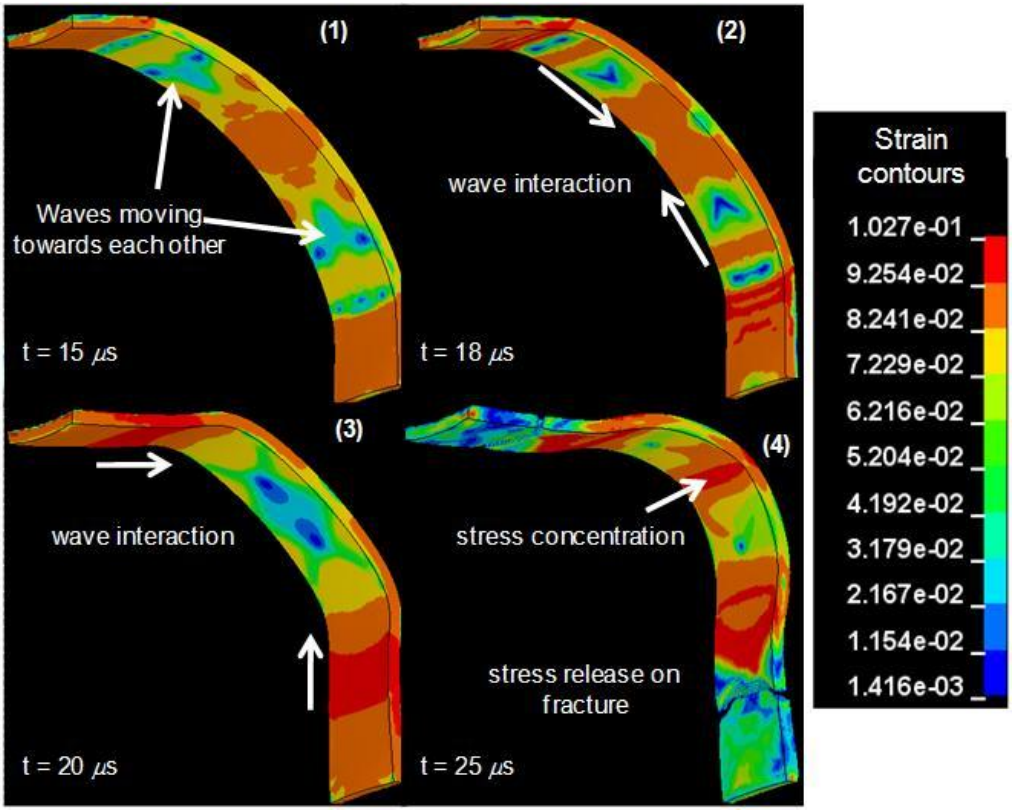

Figure 7: *Simulation results for the ring expansion (Effective von-Mises strain contours)*

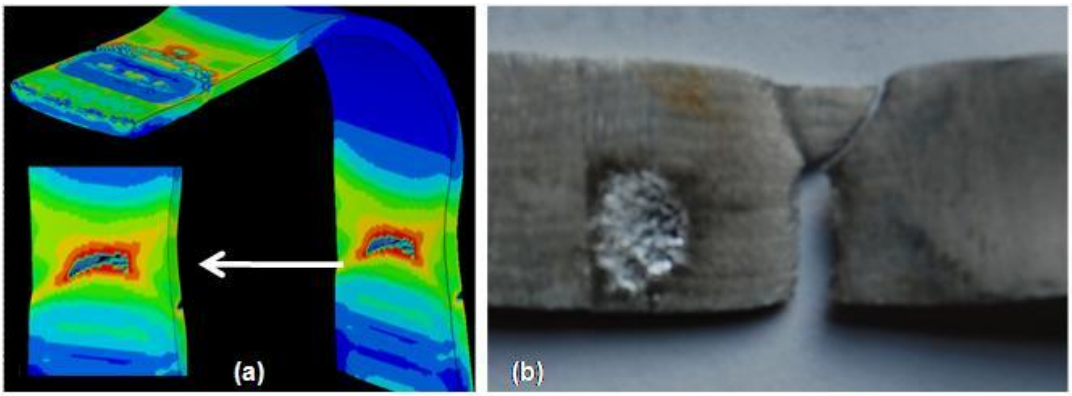

Figure 8: *X-shaped fracture patterns (a) Model (Effective von-Mises strain contours) (b) Experimental ring specimen*

4.5 Rebound Calibration

The rebound characteristics of sheet metal upon impact critically influence the shape conformity of the formed product. The qualitative comparison between the numerical model and formed specimens shown in Figure 5 reveal insights into the coupling between the electromagnetic and the mechanical process. The numerical model in general has higher rebound than the experimental product. This is because the pressure boundary condition is released upon contact to let the ring specimen fly on account of its own inertia. In reality, the specimen upon impact is stabilized against the square die by the magnetic pressure that prevents it from bouncing back. The measured velocity profiles in Figure 5 and Figure 6 show a trough followed by another peak in sync with the current profiles. The second peak is due to the magnetic pressure. The simulation model does not adequately portray this peak and shows a steady decline and manifests as a rebound. At low energy (5.6 kJ) the magnetic pressure begins its decline prior to the strike of the ring specimen (compare second peak in Figure 5 (a)). At 7.2 kJ, the second peak in velocity precedes that in current thus stabilizing the rebound effect and producing flatter parts. The magnetic pressure thus holds the part firmly against the die dissipating its kinetic energy into stress waves that traverse the circumference of the specimen.

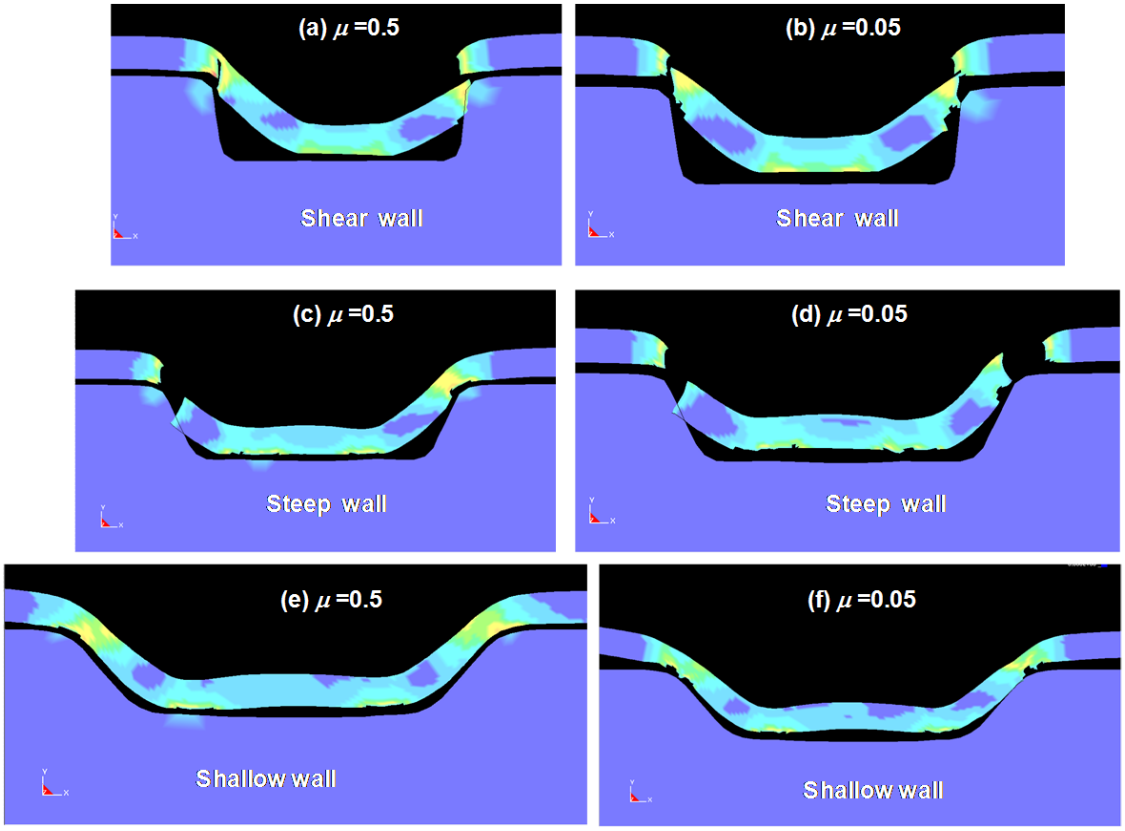

Figure 9: *Effect of entry wall angle and frictional coefficient (μ) on formed workpiece*

4.6 Effect of entry wall angle

The quality and shape of the formed sheet metal is highly dependent upon the entry wall angle of the die channels. A steeper angle increases the propensity for shear under high

speed impact. A shallower angle is beneficial for good shape conformity as shown in *Figure 9* (e) and (f). The effect of friction has been established from section 2.4. From *Figure 9* (c) and (d), it is evident that there is higher kinetic energy in the plate that causes material to flow into the cavity and consequently shear at the edges. For these cases, a secondary forming operation is essential to ensure better shape conformity.

5 Conclusions

1. In impact forming the shape of the component can vary significantly from the shape of the die upon which the sheet strikes. This is influenced by rebound of the specimen upon impact, friction between interfaces, geometry of the die (including the stiffness of the component produced) and the persistence of magnetic pressure after die strike. Rebound can be minimized by plastically dissipating the kinetic energy of the workpiece.
2. The ability to make a given shape with a specific material is closely related to frictional conditions in impact forming, as it is in traditional quasi-static forming. However, in impact forming high coefficients of friction are generally favored because draw-in is difficult in impact forming. The design strategy is to have each material segment maintain a path along its launch vector.
3. Failure mechanisms are attributed to interaction between stress and/or displacement waves, rapid change in stress states that lead into necking and consequent failure.
4. The entry wall angle plays a critical role in the shape conformity of sheet metal. For vertical shear walls, the formed shape is very different from the metal die shape. For steep angles a secondary forming operation is beneficial in improving the conformity.

References

[1] *Kamal, M. and G. S. Daehn.:* A Uniform Pressure Electromagnetic Actuator for Forming Flat Sheets." Journal of Manufacturing Science and Engineering 129(2): p.369, 2007

[2] *Strand, O. T., D. R. Goosman, et al.* Compact system for high-speed velocimetry using heterodyne techniques. Review of Scientific Instruments 77(8), p.083108., 2006

[3] *Johnson, G. R. and W. H. Cook*. Fracture characteristics of three metals subjected to various strains, strain rates, temperatures and pressures. Engineering Fracture Mechanics 21(1),p.31-48.,1985

[4] *Liang, R. and A. S. Khan*. A critical review of experimental results and constitutive models for BCC and FCC metals over a wide range of strain rates and temperatures. International Journal of Plasticity 15(9),p.963-980.,1999

[5] *Wang, Y. and Y. Xia*. Modeling of mechanical behavior of brass at high strain rates. Journal of Materials Science Letters 22(20),p.1393-1394.,2003

[6] *Banik, K. E.* Factors effecting electromagnetic flat sheet forming using the uniform pressure coil., Thesis, Ohio State University, 2008.

[7] *Kamal, M., J. Shang, et al.* Agile manufacturing of a micro-embossed case by a two-step electromagnetic forming process. Journal of Materials Processing Technology 190(1-3),p.41.2007

[8] *El-Azab, A., M. Garnich, et al.* Modeling of the electromagnetic forming of sheet metals: state-of-the-art and future needs. Journal of Materials Processing Technology 142(3),p.744.,2003

[9] *El-Azab, A., M. Garnich, et al.* Modeling of the electromagnetic forming of sheet metals: state-of-the-art and future needs. Journal of Materials Processing Technology 142(3),p.744.2003

[10] *Hu, X. and G. S. Daehn*. Effect of velocity on flow localization in tension. Acta Materialia 44(3),p.1021-1033.,1996

[11] *Imbert, J. M., S. L. Winkler, et al.* The Effect of Tool--Sheet Interaction on Damage Evolution in Electromagnetic Forming of Aluminum Alloy Sheet. Journal of Engineering Materials and Technology 127(1),p.145.,2005